Bolometric Measurements and the Role of Radiation in Alcator Power Balance

L.S. Scaturro[†] and M.M. Pickrell

Francis Bitter National Magnet Laboratory and Plasma Fusion Center
Massachusetts Institute of Technology, Cambridge, MA.   02139

[†]Also Department of Nuclear Engineering, M.I.T.

Bolometric Measurements and the Role of Radiation
in Alcator Power Balance

L.S. Scaturro[†] and M.M. Pickrell

Francis Bitter National Magnet Laboratory and Plasma Fusion Center
Massachusetts Institute of Technology, Cambridge, MA.   02139

Abstract

A bolometric study of global power balance on the Alcator A tokamak has shown that neither high nor low Z impurities play a dominant role in plasma energy confinement for "well-behaved" discharges. Spatially and temporally resolved measurements of the power lost in radiation and particles has shown that in the region 0 cm < r < 3 cm these loss mechanisms account for only 15% of the local ohmic power input. The radiative losses from the central plasma regions are attributed to molybdenum. Variation of the emissivity with density has shown that radiative and particulate losses become more important at densities less than $2 \times 10^{14} cm^{-3}$. A study of disruptive discharges and discharges showing anomalous increases in the plasma resistance has shown that radiation can be the dominant loss mechanism under these conditions.

[†]Also Department of Nuclear Engineering, M.I.T.

Bolometric Measurements and the Role of Radiation
in Alcator Power Balance

L.S. Scaturro[+] and M.M. Pickrell

Francis Bitter National Magnet Laboratory and Plasma Fusion Center
Massachusetts Institute of Technology, Cambridge, MA.   02139

[+] Also Department of Nuclear Engineering, M.I.T.

I. Introduction

Measurements of the radiative and particulate power loss in tokamaks[1,2,3] have shown that these loss mechanisms can play an important role in plasma confinement. A summary of results from many tokamaks is contained in reference 4. In particular, information regarding the spatial distribution of the radiative power loss has provided information about impurity control and effects.[5] This spatial information was obtained by scanning the plasma on a shot-to-shot basis thus making discharge reproducibility an important factor.

The diagnostic apparatus described for Alcator employs four collimated bolometers that measure the accumulated energy incident upon their surfaces during a tokamak discharge. This system allows both spatial and temporal resolution for a single discharge, which is important from the standpoint of reproducibility, and allows comparison with spectroscopic measurements[6] of the plasma emission coefficient near the edge. The following topics will be discussed: (I) Description of the experimental apparatus and technique, (II) Spatial and temporal behavior of the plasma emission coefficients and power loss for typical Alcator discharges, (III)Variation of the power loss at "steady-state" plasma conditions with density, and a comparison of data with spectroscopic and soft x-ray measurements and theoretical calculations (IV) A simple power balance picture, (V) Power loss associated with disruptions and plasmas exhibiting resistive anomalies.

I) Experimental Description

The bolometer system consists of four berrylium oxide discs[7] with thermistor material sintered onto the back surface and gold-black evaporated onto the front, plasma-facing surface. These discs are mounted at the end

of blackend collimating tubes that view different spatial regions of the plasma from top to bottom as shown in figure 1. The chordal positions of the bolometers are h = 0 cm, h = -3.3 cm, h = 4.5 cm and h = 8.8 cm, viewing regions that afford a spatial resolution of 2 to 3 cm. The discs are 1.9 cm in diameter and 0.0254 cm thick. The thermistor material is monitored for resistance changes by a self-balancing bridge network that can detect changes in the substrate temperature as small as 1×10^{-3}°C. The measured rise time of the detectors is approximately 1.2 msecs and cooling time in vacuum is longer than ten seconds. The bridge output voltage is a linear function of the substrate temperature and therefore directly proportional to the total accumulated energy incident on the bolometer.

The gold-black coating gives essentially 100% absorbance of incident radiation with wavelengths smaller than 20 μm.[8] For very short wavelengths, the substrate starts to become transparent to photons with energies greater than 6 keV. Assuming a 100% absorption coefficient over the entire spectral range, a responsivity for each bolometer is calculated to be 0.144 Volts/mJoule. This number agrees quite well with two separate calibrations performed for each bolometer; one calibration with a mercury arc lamp and one with a 3200°C tungsten-halide lamp. The average value for responsivity measured in these calibrations, which were referenced to an electrically calibrated power meter, was 0.137 Volts/mJoule with a standard deviation of approximately 0.006 V/mJoule.

After a plasma discharge, signals from the bolometer array are digitized and stored on magnetic tape for later retrieval and analysis. A three-region inversion technique is then used to caluculate the average plasma emission coefficient as a function of minor radius for the regions 0 cm < r < 3 cm

3 cm < r < 7 cm and 7 cm < r < 11 cm. Changes in the position of the center

of the plasma current channel are taken into account by monitoring this

position with a cos θ coil and folding this information into the inversion.

Motion of the emission profile can be inferred from the raw bolometer

signals, but the bolometers positioned at h = -3.3 cm inside and h = 4.5 cm

outside proved to be too close in chordal position to produce a non-oscillating

four point inverted profile for every discharge. They were used to determine

information regarding the in-out symmetry of the emission profile, and to

determine the errors associated with plasma position changes (see Appendix).

II) Temporal Behavior of the Emission Coefficients

In this section, and the two following sections, data will be presented

only for well-behaved discharges. These discharges are characterized by a

resistive loop voltage consistent with $Z_{eff} \approx 1$,[9] the absence of MHD activity

as detected by $\dot{B}$ loops and the presence of well developed sawteeth in the

central soft x-ray emission. Oscillograms showing data from this type of

discharge are shown in figure 2. Inverted data for this type of discharge

are shown in figure 3 where the central, middle and edge region emission

coefficients are plotted as a function of time along with the loop voltage,

plasma current and line-averaged electron density. Due to smoothing

necessary for signal processing, the time resolution for these inverted

profiles is approximately 10 msecs. The total power output derived from

summing the emission from all spatial regions is also plotted. From this

it can be seen that the power output scales fairly closely with density at

densities above $\bar{n}_e = 1 \times 10^{14} cm^{-3}$, and reaches a fairly constant value

when the density is constant. During the "steady-state" conditions the

density in the limiter shadow region is actually falling,[10] and this may

account for the decrease in the edge emission coefficient during this time. During the density rise portion of the discharge, about 20% of the ohmic input power is used to ionize and heat the plasma. The large increase in emission coefficients at the end of the discharge is due to the fact that current channel is shrinking and the temperature is falling. This comes about because the power supply is inverting the voltage on the primary of the ohmic heating transformer. This portion of the discharge is not well analyzed.

III) <u>Variation of the Emission Coefficients with Density During "Steady-State" Plasma Conditions</u>

Figure 4 shows bolometrically determined emission coefficients for the three spatial regions and the total power loss as a function of density for B_T = 60 kG and I_p = 150 kA (q = 3.8). This compilation of data is representative of a large data base. These data are typical of well-behaved discharges and represent the fluctuation in shot-to-shot power loss for seemingly identical discharges. Of course, the energy confinement time is not measured directly on a shot-to-shot basis and could also reflect these fluctuations.

The edge emission coefficient ε_3 (7 cm < r < 11 cm) increases with density from $\bar{n}_e$ = 2.5 x 10^{14}cm^{-3} to 4.5 x 10^{14}cm^{-3} and in this density range is due to nitrogen, carbon, hydrogen, and oxygen line emission.[6] The magnitude and variation of the emission coefficient in this region agrees well with that inferred from spectroscopic measurements[6] of light impurities. At densities less than 2 x 10^{14}cm^{-3} ε_3 increases as the density decreases. Since light impurity levels continue to decrease[11] in this range,

this effect may be due to a decreasing plasma opacity to charge-exchange neutrals[12] and therefore may represent a shift from a radiative energy loss to a particulate energy loss mechanism in this region.

The middle region emission coefficient ϵ_2 (3 cm < r < 7 cm) shows the same type of qualitative behavior as the edge, and at densities less than 2.5 x 10^{14} cm^{-3} increased charge-exchange losses may account for the increase in emission.

The central emission coefficient ϵ_1 (0 cm < r < 3 cm) increases with denisty from 1 x 10^{14} cm^{-3} to 4.5 x 10^{14} cm^{-3}. The absence of an increase in the emission at lower densities is probably due to the fact that the neutral source term at the center is too small for there to be a substantial charge-exchange power loss from this central region.

At high densities ($\bar{n}_e \geq$ 2 x 10^{14} cm^{-3}) the central ϵ_3, and middle region, ϵ_2, emission coefficients have values near 1 - 2 Watts/cm^3. This magnitude of emission can be caused by line radiation from high Z impurity atoms. Following is an argument that shows that molybdenum impurity atoms, (limiter material) in reasonable number, can account for this magnitude of power loss.

The density of molybdenum in the central and middle regions can be estimated from the measured emission coefficients and theoretical calculations of the total power radiated in Mo line emission from a plasma of known electron temperature T_e. The average Mo density can be computed from

$$\langle n_{Mo}\rangle\Big|_0^{3\ cm} = \frac{\epsilon_1\ [\text{Watts/cm}^3]}{\langle n_e\rangle\Big|_0^{3\ cm} L_{Mo}\ (T_e)}$$

where ϵ_1 is the measured emission coefficient, $\langle n_e\rangle\Big|_0^{3\ cm}$ is the average electron density in the region 0 < r < 3 cm, $\langle n_{Mo}\rangle\Big|_0^{3\ cm}$ is the average molybdenum density in this region and $L_{Mo}\ (T_e)$ is the radiative cooling

rate according Post and Jensen.[13] This rate is fairly independent of temperature in the range 400 eV < T_e < 1 keV, which is of interest for Alcator.[9] Figure 5 is a plot of the density of Mo for the central and middle regions as a function of line averaged electron density. At $\bar{n}_e$ = 3.5 x 10^{14}cm^{-3} the central Mo density represents a fractional concentration of only 3 x 10^{-5}. It can be seen from this figure that there is no accumulation of high Z impurities in the central plasma region. Also plotted on this graph is the Mo density inferred from soft x-ray measurements of a Mo L transition line near 2.7 KeV.[14] This data was taken simultaneously with the bolometric measurements. The agreement is good at high densities, but diverges at lower densities. Part of this discrepancy comes from the fact that the x-ray diagnostic makes a line-averaged intensity measurement through a central chord on a single shot and therefore reflects the line averaged molybdenum density. At low densities there may also be some error in the assumption that the total power loss from the central regions is due to Mo radiation, when in fact part of the emission could come from other loss mechanisms.

The magnitude of the edge region emission coefficient agrees well with that inferred from spectroscopic measurements of low Z impurities[6] (nitrogen, oxygen, carbon). However, if the molybdenum density is fairly constant across the plasma radius, then this edge emission coefficient would have to be twice as large as the measured value to also account for the high Z molybdenum radiation. The accuracy of the cooling rate calculations, however, at temperatures below 200 eV, which are characteristic of this edge region, is poor.[13] It is therefore concluded that in this region (10 eV < T_e < 150 eV) molybdenum is not an efficient radiator.

IV) A Simple Power Balance

For an Alcator discharge where $\bar{n}_e = 3.5 \times 10^{14} cm^{-3}$, $I_p = 150$ K Amps and $B_T = 60$ kG, approximately 40% of the total power input is lost in radiation during steady state conditions. This number, however, is not directly related to the energy confinement picture since the spatial region form which this power is lost determines the effect on the discharge energy confinement time. Figure 6 shows a power flow diagram during steady-state plasma conditions for this type of Alcator discharge. Three spatial regions are shown. The numbers given for each region are average values for that region and the ohmic power inputs were derived from laser scattering measurements[15] of the electron temperature profile and measurements of the resistive loop voltage. As can be seen, the central emission coefficient represents about 25% of the total power input to that region ($P_{conduction} + P_{ohmic}$), and the edge emission is about 32% of the total power input there. It is believed that the remainder of the energy is conducted to the limiter, but while the limiter does heat up during a discharge, a reliable estimate of the total energy flow to the limiter cannot be made at this time.

V) Resistive and Disruptive Discharges

Many Alcator discharges do not produce the well-behaved plasma conditions documented in the preceeding sections. Unfortunately, these pathological cases are difficult to study both because of their irreproducibility and because of the rapidly changing plasma conditions. In this section a simple description in terms of power balance will be given for both disruptive and resistive discharges.

Oscillograms for a discharge terminated by a total disruption are shown in figure 7. This type of discharge shows no evidence of disruption before termination on the time-scale of observation ($\tau \sim 1$ msec), i.e., the resistive loop voltage, soft x-ray emission and plasma current show no anomalous effects. A negative voltage soike, followed by a positive voltage spike occurs, the plasma current then terminates in less than two to three milliseconds and a total disruption occurs. The bolometer signals show large jumps in the energy lost from the plasma in radiation and charge-exchange neutrals from all spatial regions. An analysis of these bolometer signals shows the following energy balance picture:

Energy lost from $0 < r < 3$ cm	= 480 KJ
Energy lost from 3 cm $< r < 7$ cm	= 6.5 KJ
Energy lost from 7 cm $< r < 11$ cm	= 3.0 KJ
Total energy lost	= 13.5 KJ
Plasma energy	= 3.2 KJ
Stored magnetic field energy	= 9.8 KJ
Total energy available	= 13.0 KJ

This shows that within experimental error during a major disruption both the plasma energy and the stored magnetic field energy ($\frac{1}{2} L I^2$) are lost in the form of radiation or charge-exchange neutrals. This result is consistent with the findings for ATC[2].

There is a different phenomenon that effects Alcator discharges adversely that we have termed a "resistive bump". Figure 8 shows oscillograms for a discharge that exhibits such an anomalous increase in the resistive loop voltage over a time scale of several milliseconds. Associated with this increase in voltage is an increase in the central and middle region emission, a drop in the central electron temperature, a change

in the soft x-ray emission and a decrease in energy confinement time.

Figure 9 shows inverted bolometer data that give the three emission coefficients along with the loop voltage as functions of time for a discharge exhibiting a resistive bump. The bolometer data have been smoothed in this case giving a time response of about 10 msecs. As can be seen, the emission profile becomes quite peaked on acis, as compared to the well-behaved state described in sections III & IV. Other discharges exhibit severe resistive bumps with central region emission coefficients increasing rapidly to values exceeding 20 Watts/cm^3. These discharges also show rapid cooling in the center[16] and usually terminate abruptly. They are quite different from a "disruption" which is always preceeded by a negative voltage spike and shows an associated change in dI_p/dt. There are several possible explanations for the cause of this phenomenon, of which none is complete but some quite plausible. An influx of molybdenum into the discharge is probably the most likely scenario. Since the emission coefficient shows a strong peaking on axis, and the edge emission coefficient does not change, this strongly suggests that a high Z impurity is responsible for the increased radiation, the fall of the central electron temperature, and therefore an increase in the resistive loop voltage. The total power radiated by molybdenum is relatively insensitive to electron temperature over the range of interest, so inductive effects cannot account for this increased emission. Therefore there must be a change in the molybdenum density in the central region. The mechanism for the molybdenum influx is not known, but possibilities include arcing and local hot spots on the limiter. Since the edge emission coefficient does not increase during this event and even shows a slight decrease, it is concluded that molybdenum is not an efficient radiator in this region where 10 eV < T_e < 150 eV.

Another method by which the central impurity density could increase would be the transport of molybdenum already in the discharge to the central region. For example, if the molybdenum density profile was flat before the occurrence of a resistive bump, and some effect caused the sudden inward transport of impurities, this could increase the central emission coefficient. If half of the molybdenum atoms in a well-behaved discharge in the region 3 cm < r < 7 cm were transported to the central region, this would increase the central emission coefficinet by a factor of ten, and could cause a resistive bump. The proof of these conjectures awaits further experimentation including coordination with spectroscopic diagnostics and an impurity injection experiment.

IV Conclusions

Radiation from high and low Z impurity ions does not play a dominant role in energy confinement in well-behaved high-density Alcator diacharges. For the central plasma "core", radiation plays an insignificant (<15%) role in the total power balance. However, in the middle plasma region (3 cm < r < 7 cm) radiation accounts for a 25% loss of input power. Since a substantial fraction of the total plasma volume is contained in this region (45%), this power loss has some effect on the global energy confinement time. Although it does not represent the dominant energy loss mechanism, the suppression of this energy loss mechanism may result in improvements in energy confinement.

The edge plasma region (7 cm < r < 11 cm) is fairly well understood. Emission coefficients from bolometric measurements agree with those derived from spectroscopic measurements of low Z impurity emission. It is difficult to say what role this region plasys in global energy confinement because plasma-wall/limiter interactions must be taken into account,

therefore the effects of radiation in this region are hard to ascertain. Both the measurement of the power loss to a molybdenum limiter and the use of other limiter materials are planned experiments that may provide information about this region.

Lower density operation ($\bar{n}_e < 2 \times 10^{14} cm^{-3}$) is not well understood from the bolometric data available in terms of radiative and particulate power loss. The increase in the outer region emission coefficients could be due to an increased particle loss in the form of charge-exchange neutrals, but there is no good quantative arguement for this statement since a calculation of the power lost in charge-exchange neutrals depends strongly on the edge plasma temperature and edge neutral density, which are not well known. This increase in emission could also be due to an increased plasma-wall/limiter interaction and an associated increase in the impurity concentration in the outer plasma regions.

Both disruptive and resistive discharges have been studied from a global power balance viewpoint. For total plasma disruptions, which exhibit a negative voltage spike and complete current termination, both the stored magnetic field energy and the internal plasma energy are lost in the form of radiation and neutral particles. For discharges exhibiting anomalous increases in the resistive voltage, it is shown that the plasma emission coefficients in the central regions increase substantially by an amount dependent on the severity of the resistive bump. It is believed that the resistive bump phenomenon is caused by an increase in the molybdenum density due to an influx of this metal, but the mechanisms by which this influx may occur are not understood.

Acknowledgements

The authors would like to thank the entire Alcator group for their contribution to this work.

APPENDIX

A description of the spatial inversion technique and the errors associated with the bolometric diagnostic system are contained in this appendix. For this reason, error bars were omitted from the data graphs contained in the main body of this article. As mentioned in preceeding sections, on a shot-to-shot and day-to-day basis plasma impurity levels, and therefore bolometric signals, vary appreciably. However, once a well-behaved discharge condition is obtained, the shot-to-shot reproducibility is excellent. It is for these types of reproducible discharges where an error analysis is appropriate.

The error associated with calibration of the bolometer elements is under five percent, and is negligible when compared to other error sources. The largest source of error involves the inversion of the raw bolometer signals to formulate a plasma emissivity as a function of radius.

The inversion technique is a simple one where the effective volumes (including solid angle effects) viewed by each bolometer are incorporated into an inversion matrix. In order to determine the power emitted per unit volume as a function of radius the following equation is utilized:

$$\epsilon_i = \frac{d}{dt} \sum_{j=1}^{3} M_{ij} \, S_j$$

where S_j is the signal from the jth bolometer, M_{ij} is the effective volume viewed in the ith radial shell by the jth bolometer and ϵ_i is the emission coefficient associated with the ith radial shell. Poloidal symmetry is assumed. The inversion matrix coefficients are determined numerically from geometric considerations. These coefficients depend upon the position of the center of the emission profile and must be adjusted as the plasma moves with respect to the vacuum vessel. Two different methods were employed to determine the plasma position. A

cos θ wound magnetic coil was used to monitor the position of the center of the current channel and the four raw bolometer signals, utilizing a curve-fitting technique, were also employed to give plasma position. The positions derived by these two methods were used as input to determine the appropriate inversion matrix coefficients. The spread in the calculated emissivities using the two different techniques is typical of the maximum error. During "steady-state" plasma conditions the position derived from the two different techniques agreed to within ten percent, but was larger during discharge initiation or termination.

These techniques have shown that maximum changes and uncertainties associated with the plasma position can cause errors in the central emissivity ϵ_1 on the order of $\pm$ 50%. For the middle region emissivity ϵ_2 this error is $\pm$ 30% and for the edge region ϵ_3 the error is $\pm$ 20%. The inclusion of the errors mentioned here would not affect the conclusions of the main text.

REFERENCES

1   Gorelik, L.I., Razumova, K.A., Sinitsyn, V.V. in Plasma Physics
     and Controlled Fusion Research (Proc. Conference Culham, 1965)
     2, IAEA, Vienna (1966) 647.

2   Hsuan, H., Bol, K., Ellis, R.A., Nuclear Fusion 15, (1975) 657.

3   Bush, C.E., Lyon, J.F., ORNL/TM-6148 (1977).

4   Edmonds, P.H., England, A.C., Nuclear Fusion 18, (1978) 23.

5   Grisham, L., Hsuan, H., Schmidt, G., Bull. Am. Phy. Soc. 23, No. 7
     (1978) 797.

6   Terry, J.L., Chen, K.I., Moos, H.W., Marmar, E.S., Nuclear Fusion 18,
     (1978) 485.

7   Manufactured by Victory Engineering Corporation, Springfield, New Jersey.

8   Smith, R.A., Jones, F.E., Chasmar, R.P., "The Detection and Measurement
     of Infra-red Radiation", Oxford University, London, (1957), 89.

9   Gaudreau, M., Gondhalekar, A., Hughes, M.H., Overskei, D., Pappas, D.S.
     Parker, R.R., Wolfe, S.M., Apgar, E., Helava, H.I., Hutchinson, I.H.,
     Marmar, E.S., and Molvig, K., Phys. Rev. Lett, 39, No. 2 (1977) 1266.

10   Scaturro, L.S., and Kusse, B., Nucl. Fus. 18, No. 12 (1978) 1717.

11   Terry, J.L., Private Communication.

12   Hughes, M.H., and Post, D.E., Princeton Plasma Physics Laboratory
     Report 1335 (1976).

13   Post, D.E., Jensen, R.V., Tarter, C.B., Grasberger, W.H., and
     Lokke, W.A., Atomic Data and Nucl. Tables 20, No. 5 (1977) 397.

REF. <u>cont.</u>

14   Rice, J.R., Private Communication.

15   Gondhalekar, A., Overskei, D., Parker, R.R., West, J., MIT,
        Plasma Fusion Center Report PFC/RR-78-15 Dec. (1978).

16   Hutchinson, I.H., Private Communication.

LIST OF FIGURES

FIG. 1) Schematic representation of bolometer viewing geometry and numbering system. The Alcator vacuum vessel and magnetic limiter shadow are shown to scale. The bolometer array is located 90° toroidally from the limiter.

FIG. 2) Oscillograms representing a typical plasma discharge in Alcator. Three bolometer signals are shown (the output voltage is directly proportional to the accumulated energy flux; negative voltage indicates positive energy flux) along with the laser interferometer signal, plasma current, central soft x-ray emission, and the resistive loop voltage. For this discharge B_T = 60 KG.

FIG. 3) Inverted bolometric data showing the three plasma emissivities ε_1, 0cm < r < 3cm, ε_2, 3cm < r < 7cm and ε_3, 7cm < r < 11cm as functions of time and the total power output. Also plotted for this discharge is the loop voltage, plasma current and line averaged electron density.

FIG. 4) Plots of the three radial emission coefficients and the total power output as a function of line-averaged electron density. These data represent steady-state plasma conditions where B_T = 60 KG, I_p = 150 kAmp(q_L = 3.8).

FIG. 5) Plot of the molybdenum density in two different spatial regions as inferred from bolometric measurements (see text) and the line-averaged molybdenum density as inferred from soft x-ray emission measurements as a function of line-averaged electron density.

FIG. 6) Schematic of radial power flow during steady-state plasma conditions where n_e = 3.5 x 10^{14}cm^{-3}, I_p = 150 kAmp, B_T = 60 kG. The total ohmic input power (inferred from Thomson scattering measurements and $Z_{eff} \approx 1$) and the total power conducted into each spatial region is shown. The percentage of the total power input to a given spatial region lost in the form of radiation and particles is shown. The total power input is both the ohmic power input to that region and the conducted power to that region.

FIG. 7) Oscillograms showing a total disruption. The three bolometric signals are shown along with the line-averaged electron density, the plasma current and the loop voltage.

FIG. 8)   Oscillograms for a discharge exhibiting a resistive bump. The
          three bolometer signals are shown along with line-averaged
          electron density, loop voltage, and the soft x-ray emission
          from a central plasma chord. The plasma current was essentially
          constant during the time period of interest at a value of 150 kA
          and $B_T = 60$ kG.

FIG. 9)   Inverted data showing the emissivities ε_1, 0 cm $< r <$ 3 cm, ε_2,
          3 cm $< r <$ 7 cm, and ε_3, 7 cm $< r <$ 11 cm and the loop voltage
          for the discharge shown in figure 8, as functions of time.
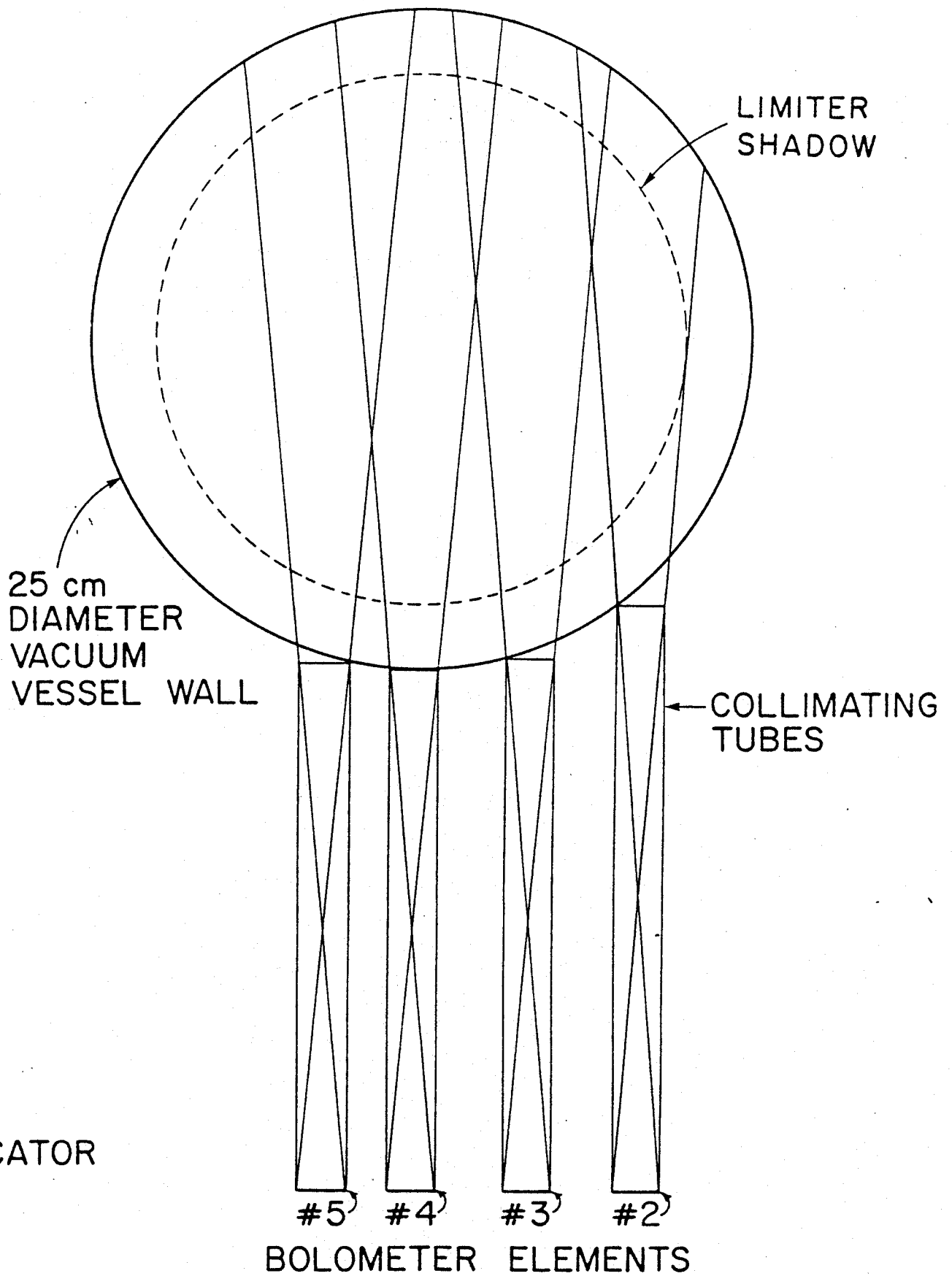
LIMITER
SHADOW

25 cm
DIAMETER
VACUUM
VESSEL WALL

COLLIMATING
TUBES

ALCATOR
C.L.

#5   #4   #3   #2

BOLOMETER ELEMENTS

BOLO NO. 4
2.8 mJ/DIV

BOLO NO. 3
3.1 mJ/DIV

BOLO NO. 2
1.1 mJ/DIV

$\bar{n}_e \left[10^{14} cm^{-3}/fringe \right]$
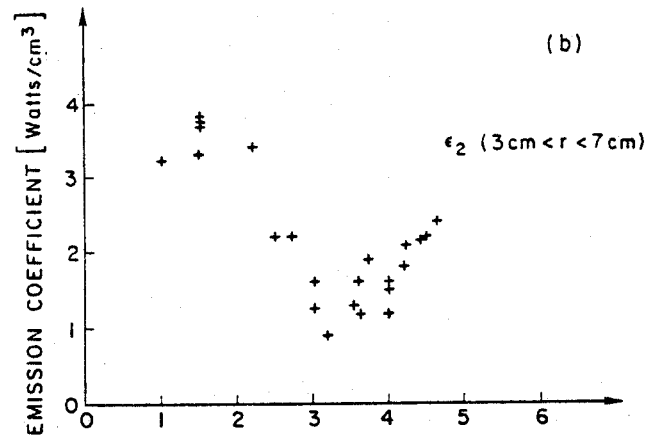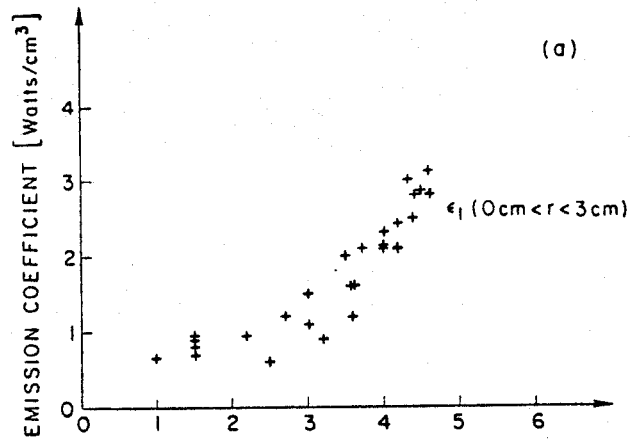
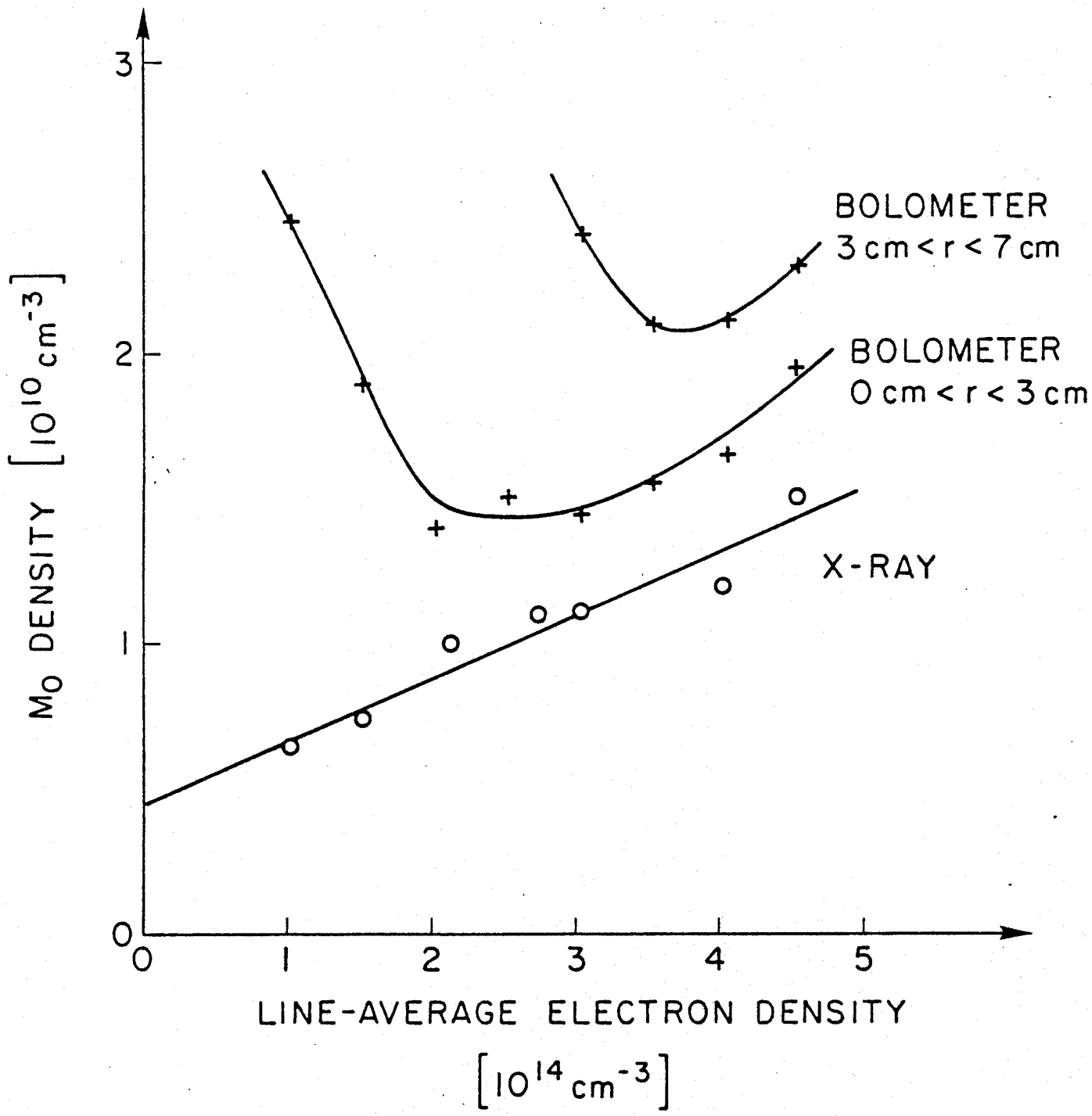PLASMA
CURRENT
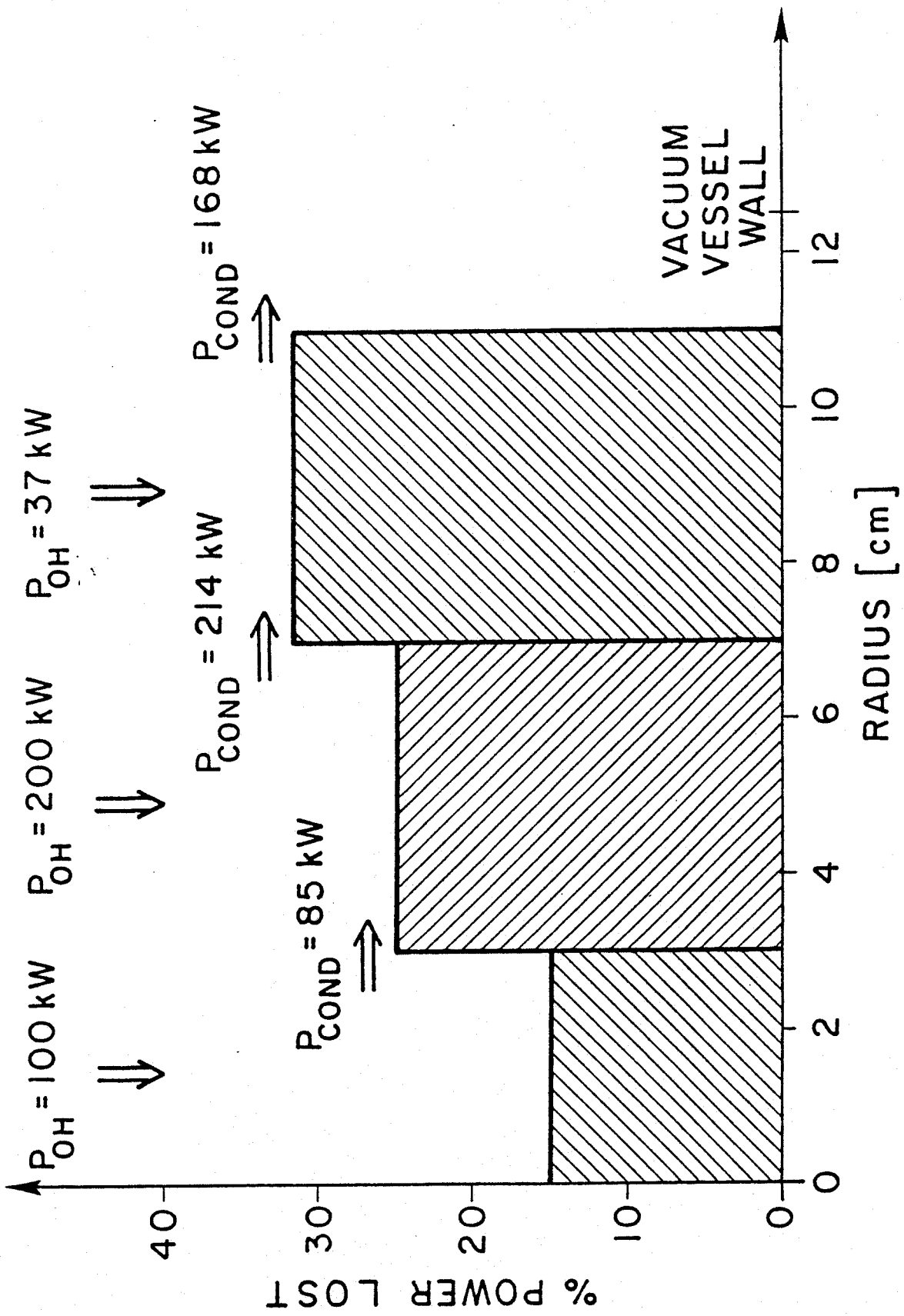[50 kA/DIV]

CENTRAL
SOFT X-RAY
EMISSION

RESISTIVE
LOOP VOLTAGE
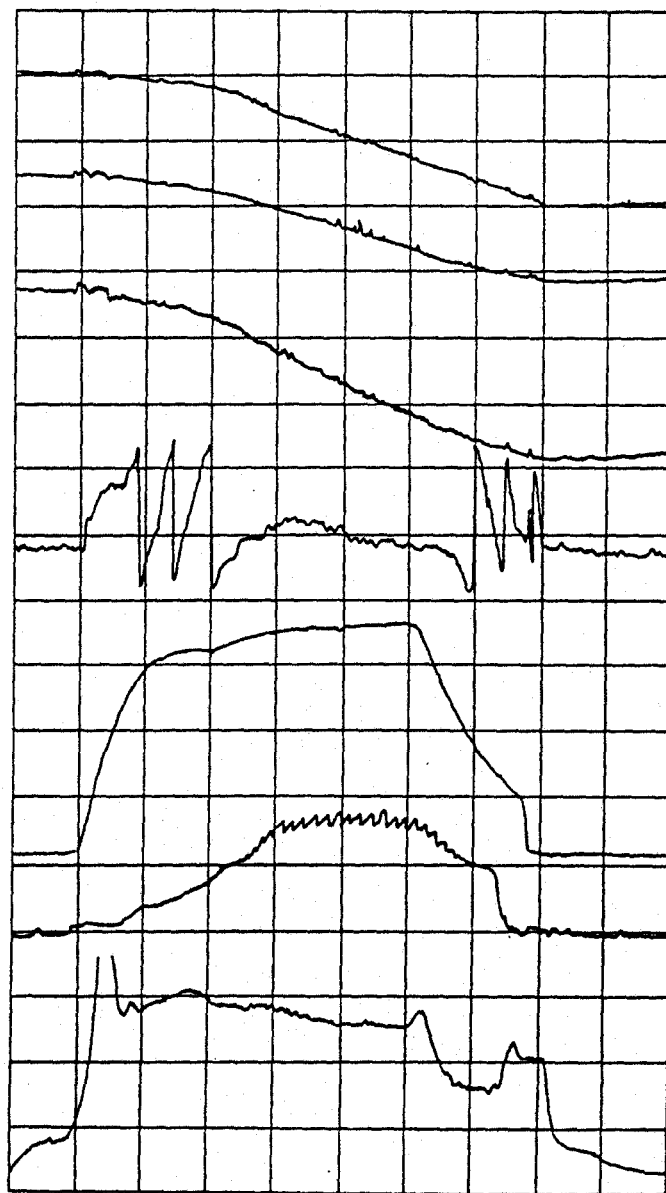
14 FEB. 79
SHOT NO. 63
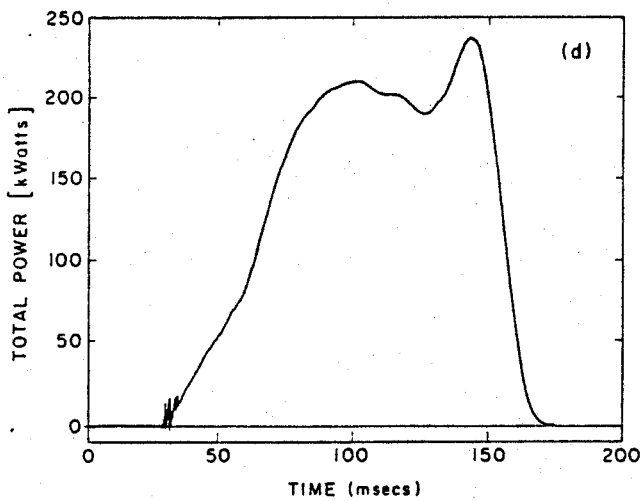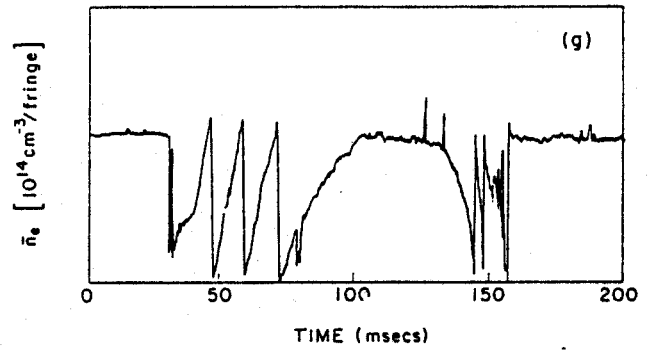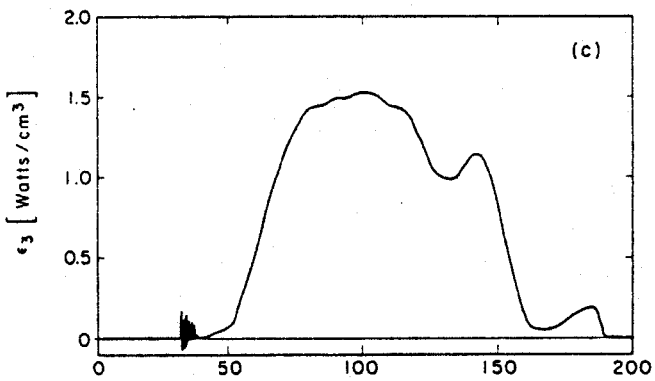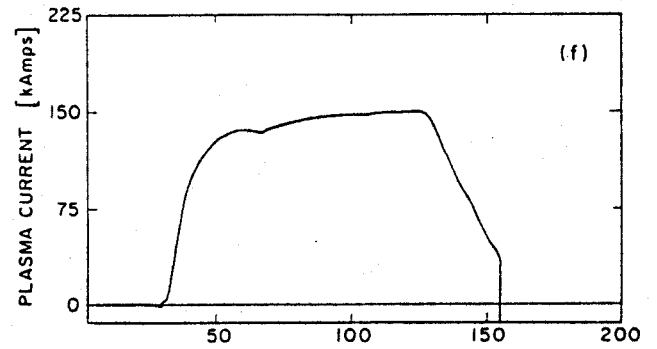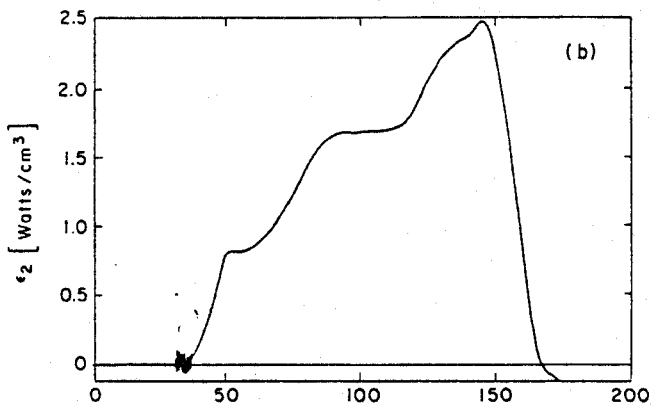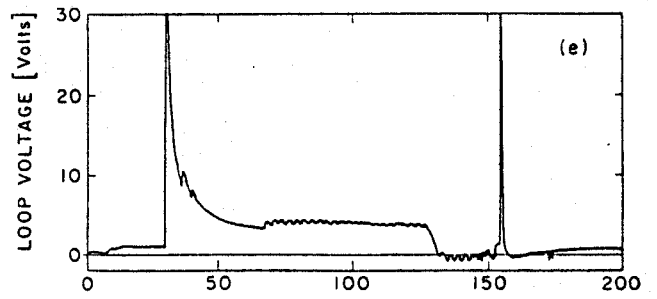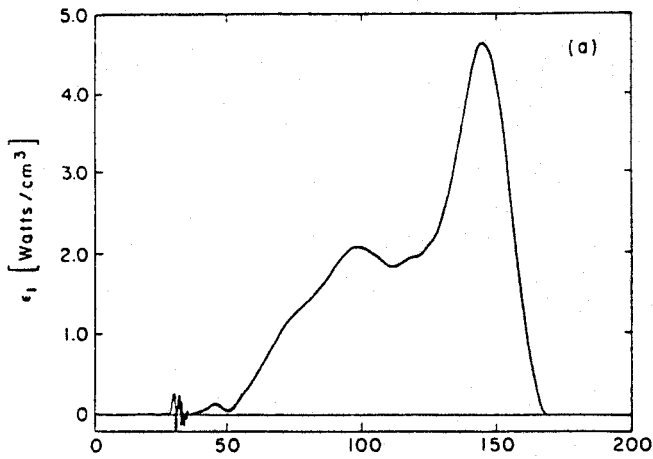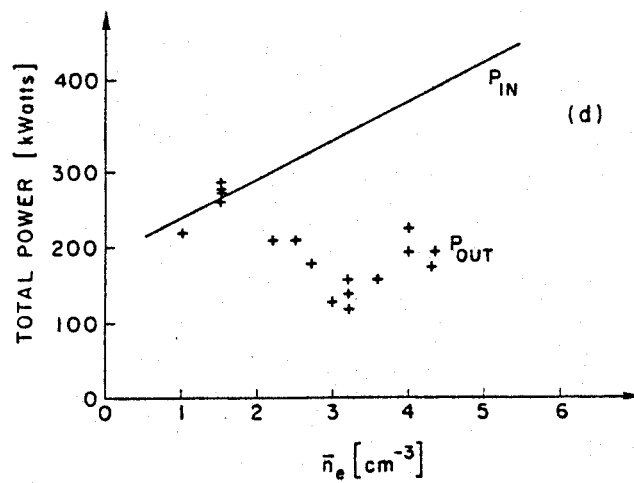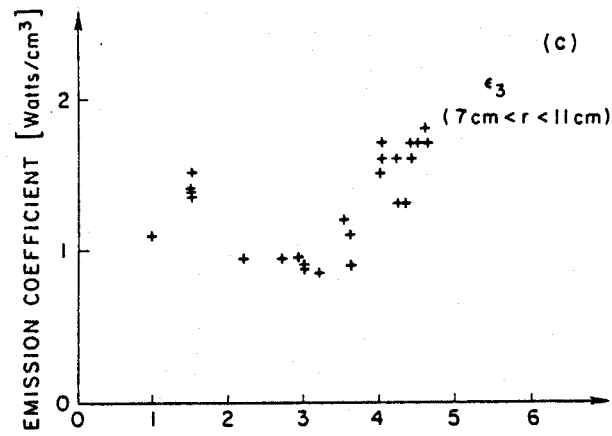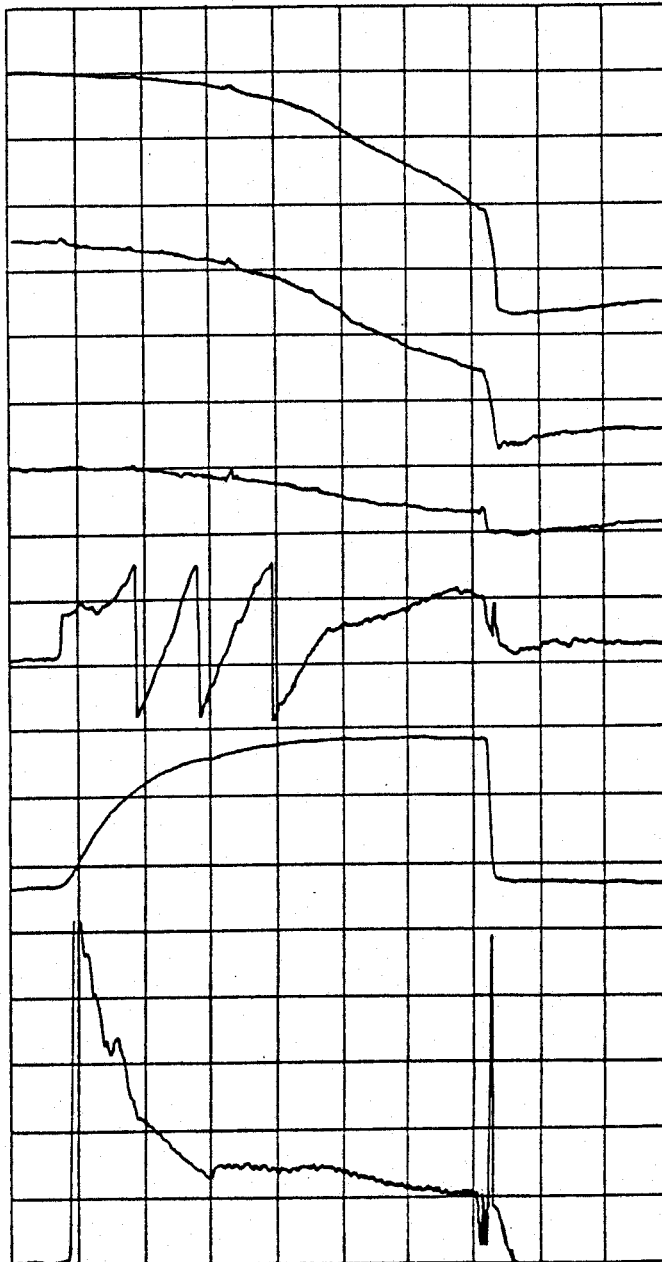
BOLO NO. 4
5.68 mJ/DIV

BOLO NO. 3
3.12 mJ/DIV

BOLO NO. 2
2.8 mJ/DIV

$\bar{n}_e \left[10^{14}\,cm^{-3}/fringe \right]$

I_p 113 kA/DIV

V_{loop} 1.3 V/DIV

6 JUNE 78
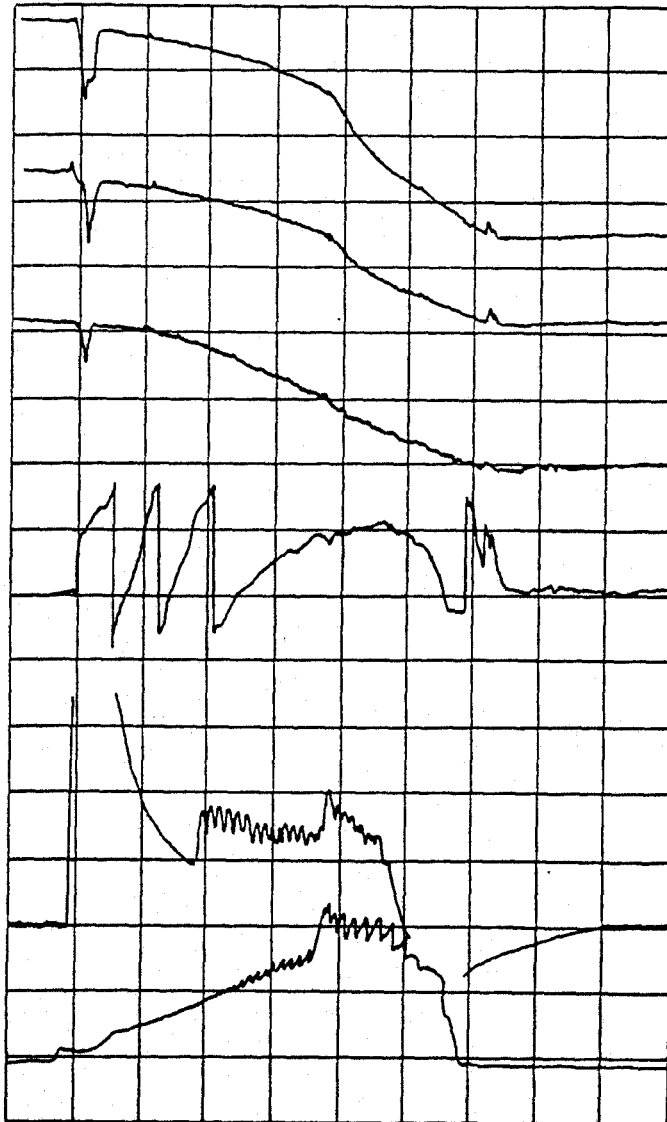SHOT NO. 29

BOLO NO. 4
2.84 mJ/DIV

BOLO NO. 3
3.12 mJ/DIV

BOLO NO.2
1.12 mJ/DIV

$\bar{n}_e \left[10^{14} cm^{-3}/fringe \right]$

V_{loop}

CENTRAL
SOFT X-RAY
DIODE

27 JAN. 79
SHOT NO. 40